

07.2

Subnanosecond AlGaAs/GaAs photodetectors with Bragg reflectors

© V.M. Andreev, V.S. Kalinovskii, G.V. Klimko, E.V. Kontrosh, A.V. Malevskaya, P.V. Pokrovskiy, M.Z. Shvarts

Ioffe Institute, St. Petersburg, Russia

E-mail: vmandreev@mail.ioffe.ru

Received April 18, 2024

Revised May 16, 2024

Accepted May 18, 2024

The paper presents the results of developing and researching highly efficient microwave laser-radiation photodetectors based on the MBE $p-i-n$ -AlGaAs/GaAs heterostructure with a Bragg reflector. The developed universal photodetectors with the photosensitive surface diameter of $70\ \mu\text{m}$ ensured obtaining the minimum FWHM photoresponse pulse duration of 135 ps in the pulsed mode at the reverse bias of 25 V. In the photovoltaic mode (without reverse bias), the efficiency factor of 60% was obtained at the laser radiation power $P_{las} = 37\ \text{mW}$ at wavelength of 850 nm.

Keywords: high-speed photodetector, molecular beam epitaxy, AlGaAs/GaAs heterostructure, Bragg reflector, pulsed laser radiation.

DOI: 10.61011/TPL.2024.09.59150.19961

Photoelectric converters (photodetectors) of laser radiation find wider and wider application in fiber-optic systems for transmitting energy via a laser beam. Wireless energy transmission over optical fiber allows for galvanic isolation of the transmitting and receiving energy modules, which provides integrated protection against electromagnetic interference. Energy transfer over an open optical channel on the Earth and in space is also promising.

Subnanosecond laser-radiation photodetectors (PDs) are important elements of radiophotonic devices transmitting high-power laser pulses [1–6]. The main requirements for such PDs are increasing the power and efficiency, as well performance. At present, AlGaAs/GaAs-heterostructure-based photodetectors operating in the spectral range of 800–860 nm are most promising for these purposes. The maximum theoretical efficiency of PD with the photoactive GaAs region is about 80% at the laser radiation power density $P_{las} = 10\ \text{W/cm}^2$ [7] and more than 85% at $P_{las} > 100\ \text{W/cm}^2$ [8]. The maximum efficiency values achieved for continuous laser radiation are 68.9% at $P_{las} = 11\ \text{W/cm}^2$ [9], 62% at $P_{las} = 100\ \text{W/cm}^2$ [10], and 54% at $P_{las} = 1400\ \text{W/cm}^2$ [11].

In this work, high spectral sensitivity in the wavelength range of $\lambda \cong 840 \pm 20\ \text{nm}$ was obtained with relatively small thicknesses of absorbing layers due to integrating into the heterostructure a Bragg reflector (BR) which reduces approximately twice the thickness of the structure's photoactive part.

The photodetector structure was grown by molecular beam epitaxy at a SemiTeq setup (Russia) on an n -GaAs substrate with dopant concentration $N_D = 3 \cdot 10^{18}\ \text{cm}^{-3}$. The structure's process scheme is given in Fig. 1, *a*.

The structure consists of a combination of AlGaAs layers of different compositions; epitaxial modes were selected for each layer individually taking into account that elements used as dopants were Si and Be. In addition to the generally

accepted epitaxial growth modes for high-quality layers of the n -GaAs base and p -GaAs:Be gradient emitter with the growth temperature elevated to 590°C , it is necessary to mention several approaches used for other structure elements.

The procedure of epitaxial growth of 12 pairs of BR layers $\{n^+-\text{AlAs}/n^+-\text{GaAs}\}$ with the base thicknesses of 69.2 and 56.1 nm, respectively, did not involve rotation of the substrate holder. Decreasing the epitaxy temperature to 500°C and reducing the arsenic flux so as to make minimal (3-fold) the ratio of fluxes of the fifth and third group elements As/Ga(Al) ensures the stoichiometric composition and planar growth of AlAs and GaAs layers and heterointerfaces, which improves the BR characteristics.

The n -GaAs base, p -GaAs:Be gradient layer and $p^+-\text{Al}_{0.12}\text{Ga}_{0.88}\text{As}$:Be layer were created at a twofold increased epitaxial growth rate (up to $1.2\ \mu\text{m/h}$) with a proportionally increased impurity flux, which reduces the growth time and likelihood of introducing foreign impurities. The $p^0-p^+-\text{GaAs}$ ($1 \cdot 10^{16} - 2 \cdot 10^{18}\ \text{cm}^{-3}$) layer with the gradient Be content was created by linearly increasing the temperature of the Be molecular beam source. To reduce the Be impurity diffusion from the heavily doped near-contact layers $p^+-\text{Al}_{0.6}\text{Ga}_{0.4}\text{As}$:Be and $p^{++}-\text{GaAs}$:Be, the growth temperature was decreased to 450°C .

Post-growth operations [10] included fabrication of a solid ohmic contact to the substrate back side, fabrication of a frontal ring contact with the photosensitive surface diameters of 70, 250 and $500\ \mu\text{m}$, removal of a part of the p -GaAs contact layer in the areas free of contacts, and application of antireflection coating.

In the fabricated PD structure there was ensured reduction in the optical, recombination and ohmic losses. Recombination losses in the p -GaAs emitter were reduced by decreasing its thickness to $0.4\ \mu\text{m}$ and creating a „pulling“ electric field by forming a gradient in the dopant

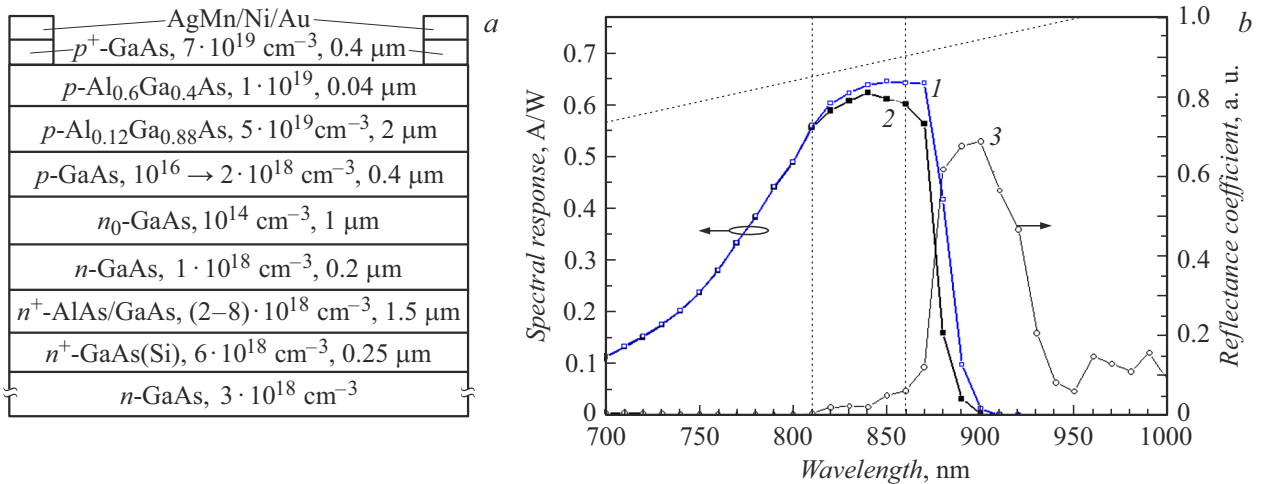


Figure 1. *a* — schematic diagram of the photodetector structure; *b* — spectra of the photodetector internal (1) and external (2) photosensitivity and reflection coefficient (3).

concentration. In the space charge region of the $p-i-n$ -junction, an i layer $1\ \mu\text{m}$ thick was grown from undoped n -GaAs ($n_0 \geq 10^{14}\ \text{cm}^{-3}$), which ensured a significant reduction in the junction capacitance. Recombination losses in the n -GaAs ($N_D = 1 \cdot 10^{18}\ \text{cm}^{-3}$) base layer get reduced due to its thickness of $0.2\ \mu\text{m}$ and presence of BR in the structure.

Reduction of ohmic losses at the dissipation resistor is ensured by low resistivity of the heavily doped ($p = 5 \cdot 10^{19}\ \text{cm}^{-3}$) front layer of $p\text{-Al}_{0.12}\text{Ga}_{0.88}\text{As}$. Reduction of the frontal ohmic „contact“ losses is ensured by increasing the doping level of the subcontact p -GaAs layer to $N_A = 7 \cdot 10^{19}\ \text{cm}^{-3}$ and creating multilayer AgMn/Ni/Au contacts providing reduction in the p -contact resistivity to $5 \cdot 10^{-6}\ \Omega \cdot \text{cm}^2$.

Spectral photosensitivity of the fabricated photodetectors (Fig. 1, *b*) was studied on test samples $2.28 \times 2.28\ \text{mm}$ in size. The maximum external spectral photosensitivity was $\text{SR}_{\text{ext}} = 0.619\ \text{A/W}$ at $\lambda = 840\ \text{nm}$ (curve 2 in Fig. 1, *b*). The surface reflection coefficient of the photodetector with the $\text{TiO}_2/\text{SiO}_2$ anti-reflection coating was 2.3% at the wavelength of 840 nm. The reflection coefficient increase to $K_{\text{refl}} > 60\%$ at $\lambda \cong 900\ \text{nm}$ is associated with the processes of laser radiation reflection and interference from the BR layers (curve 3 in Fig. 1, *b*).

The photodetector parameters (open-circuit voltage V_{oc} , fill factor FF , efficiency) were studied under irradiation with laser pulses at the radiation wavelength of 850 nm, pulse duration of 300 ns, and frequency of 1 kHz. The laser radiation power injected into the photodetector was determined based on the spectral current-power characteristic $\text{SR} = 0.604\ \text{A/W}$ at the radiation wavelength $\lambda = 850\ \text{nm}$.

Fig. 2 presents parameters of the photodetector with the photosensitive surface diameter of $70\ \mu\text{m}$ versus the laser radiation power in the photovoltaic (without reverse bias) operating mode. The maximum efficiency of 60% (curve 3 in Fig. 2, *b*) gets achieved at laser radiation power

$P_{\text{las}} = 37\ \text{mW}$. Therewith, the load characteristic filling factor is $FF = 80\%$ (curve 1 in Fig. 2, *b*), and open-circuit voltage is $V_{oc} = 1.24\ \text{V}$ (Fig. 2, *a*).

The wavelength of 850 nm is not optimal for the structure under study. The spectral photosensitivity maximum is located at wavelength $\lambda = 840\ \text{nm}$ and is $\text{SR} = 0.619\ \text{A/W}$. The calculated maximum efficiency reaches 61.4% (curve 2 in Fig. 2, *b*).

Performance of the developed photodetectors was studied for samples with the photosensitive surface diameters of 70, 250 and $500\ \mu\text{m}$ irradiated with laser pulses 10 ps in duration at the wavelength of 780 nm. In contrast to the above-described photodetector efficiency studies performed in the PD photovoltaic mode (without external bias), studies of the PD performance were carried out at the reverse bias voltage of 25 V; this ensured matching of the PD internal resistance with the measuring circuit load resistance. The measuring circuit involves photodetector, load resistor ($50\ \Omega$) and reverse bias source connected in series. Pulsed voltage generated across the load was recorded with an oscilloscope with the bandwidth of 7 GHz and input impedance of $50\ \Omega$. Thus, the total load resistance was $25\ \Omega$.

In addition to matching with the load, the photodiode operating mode with external reverse bias provides the PD power increase proportionally to the increase in voltage generated across the load after applying the pulsed laser radiation. The reverse bias increase leads to an increase in the thickness of the space charge region, decrease in the photodetector capacitance and, hence, improvement in the PD performance.

By studying the capacitance-voltage characteristics of PD with the photosensitive surface diameter of $70\ \mu\text{m}$, the capacitance was found to decrease with the negative bias increasing in the range of 0–20 V: from 3.6 pF in the absence of external bias to 3 pF with the reverse bias of 20 V.

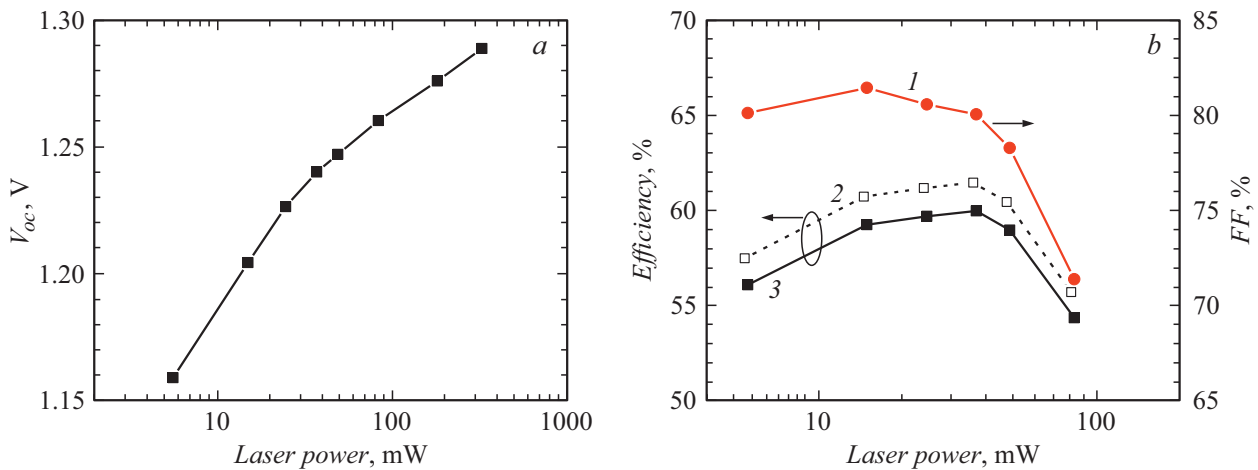


Figure 2. Photodetector parameters versus laser radiation power ($\lambda = 850$ nm). *a* — open circuit voltage V_{oc} ; *b* — fill factor FF of the load current-voltage characteristic (1), efficiency at wavelengths $\lambda = 840$ (2) and 850 nm (3).

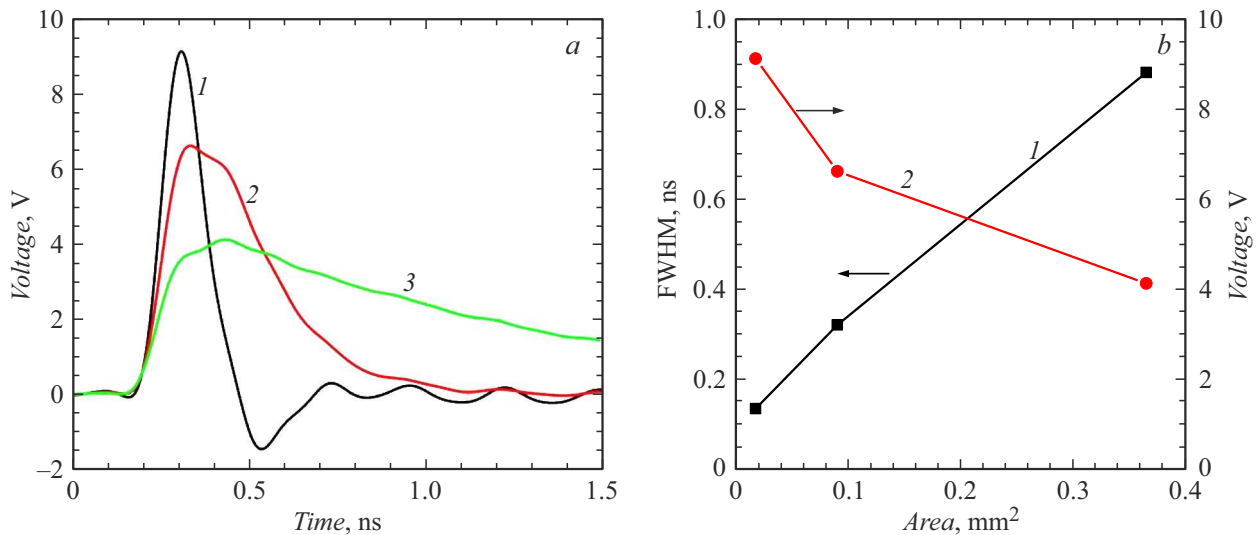


Figure 3. *a* — photoresponse pulse shapes for the developed photodetectors with the photosensitive surface diameters of 70 (1), 250 (2) and 500 μm (3) at the reverse bias of 25 V. *b* — photoresponse pulse half-width (1) and peak voltage (2) versus the photodetector p - n -junction area.

Fig. 3, *a* demonstrates the shapes of output voltage pulses across the loads of photodetectors with different photosensitive surface diameters, while Fig. 3, *b* presents the dependence of the peak voltage and duration at half-maximum of the of electrical pulse amplitudes for different photodetector areas. The minimal photoresponse pulse duration $\tau_{0.5} = 135$ ps and peak output voltage $V_{\text{max}} = 9.1$ V were obtained at the load interconnected in the circuit of the photodetector with the photosensitive surface diameter of 70 μm and reverse bias of 25 V.

Larger-area photodetectors exhibit an increase in the photoresponse pulse duration and decrease in the peak voltage. For instance, pulse durations of photodetectors with photosensitive surface diameters of 250 and 500 μm were 320 ps at the peak output voltage of 6.6 V and 885 ps at the peak voltage of 4.1 V. The increase in the photore-

sponse pulse duration and reduction in peak voltages are associated primarily with an increase in the capacitance of photodetectors with an increase in their areas.

Thus, we have developed highly efficient laser-radiation photodetectors with the photosensitive surface diameter of 70 μm , which are able to operate both in the photovoltaic mode (without reverse bias) with the efficiency factor of 60% at the radiation wavelength $\lambda = 850$ nm, and in the photodiode mode with the minimum half-amplitude voltage pulse duration $\tau_{0.5} = 135$ ps and reverse bias of 25 V. High values of spectral photosensitivity $SR = 0.619$ A/W at the wavelength of 840 nm and $SR = 0.604$ A/W at 850 nm were achieved mainly by optimizing absorbing layers parameters and creating a rear BR.

The developed photodetectors can find wide application in radio-phonic devices and other information and energy

systems for wireless optical-channel transmission of energy and information simultaneously.

Conflict of interests

The authors declare that they have no conflict of interests.

References

- [1] D. Wake, A. Nkansah, N.J. Gomes, C. Leithien, C. Sion, J.-P. Vilcot, *J. Lightwave Technol.*, **26** (15), 2484 (2008). DOI: 10.1109/JLT.2008.927171
- [2] C.G. Guan, W. Liu, Q. Gao, *Mater. Sci. Semicond. Process.*, **75**, 136 (2018). DOI: 10.1016/j.mssp.2017.11.027
- [3] R. Kimovec, H. Helmers, A.W. Bett, M. Topič, *Prog. Photovolt.: Res. Appl.*, **27** (3), 199 (2019). DOI: 10.1002/pip.3075
- [4] E. Lopez, O. Höhn, M. Schauerte, D. Lackner, M. Schachtner, S.K. Reichmuth, H. Helmers, *Prog. Photovolt.: Res. Appl.*, **29** (4), 461 (2021). DOI: 10.1002/pip.3391
- [5] M.N. Beattie, H. Helmers, G.P. Forcade, C.E. Valdivia, O. Höhn, K. Hinzer, *IEEE J. Photovolt.*, **13** (1), 113 (2023). DOI: 10.1109/JPHOTOV.2022.3218938
- [6] V.S. Kalinovskii, E.I. Terukov, Yu.V. Ascheulov, E.V. Kontrosh, V.S. Yuferev, K.K. Prudchenko, A.V. Chekalin, E.E. Terukova, I.A. Tolkachev, S.E. Goncharov, V.M. Ustinov, *Tech. Phys. Lett.*, **49** (1), 62 (2023). DOI: 10.21883/TPL.2023.01.55352.19306.
- [7] V.M. Andreev, V.A. Grilikhes, V.D. Rummyantsev, *Photovoltaic conversion of concentrated sunlight* (John Wiley & Sons, Ltd., 1997).
- [8] E. Oliva, E. Dimroth, A.W. Bett, *Prog. Photovolt.: Res. Appl.*, **16** (4), 289 (2008). DOI: 10.1002/pip.811
- [9] H. Helmers, E. Lopez, O. Höhn, D. Lackner, J. Schön, M. Schauerte, M. Schachtner, F. Dimroth, A.W. Bett, *Phys. Status Solidi (RRL)*, **15** (7), 2100113 (2021). DOI: 10.1002/pssr.202100113
- [10] N.A. Kalyuzhnyy, A.V. Malevskaya, S.A. Mintairov, M.A. Mintairov, M.V. Nakhimovich, R.A. Saliy, M.Z. Shvarts, V.M. Andreev, *Solar Energy Mater. Solar Cells*, **262**, 112551 (2023). DOI: 10.1016/j.solmat.2023.112551
- [11] A.N. Panchak, P.V. Pokrovskiy, D.A. Malevskiy, V.R. Larionov, M.Z. Shvarts, *Tech. Phys. Lett.*, **45** (1), 24 (2019). DOI: 10.1134/S1063785019010310.

Translated by EgoTranslating